Development 129, 2711-2722 (2002)
Printed in Great Britain © The Company of Biologists Limited 2002
DEV2850

Specific ablation of the nidogen-binding site in the laminin γ1 chain interferes with kidney and lung development

Michael Willem[1], Nicolai Miosge[2], Willi Halfter[3], Neil Smyth[4], Iris Jannetti[1], Elke Burghart[1], Rupert Timpl[1] and Ulrike Mayer[1,5,*]

[1]Max-Planck-Institute for Biochemistry, Department of Protein Chemistry, 82152 Martinsried, Germany
[2]Institute for Histology, University of Göttingen, 37075 Göttingen, Germany
[3]University of Pittsburgh, Department of Neurobiology, Pittsburgh, PA 15261, USA
[4]Institute for Biochemistry, University of Cologne, 50931 Cologne, Germany
[5]University of Manchester, Wellcome Trust Centre for Cell-Matrix Research, Manchester M13 9PT, UK
*Author for correspondence (e-mail: ulrike.mayer@man.ac.uk)

Accepted 18 March 2002

SUMMARY

Basement membrane assembly is of crucial importance in the development and function of tissues and during embryogenesis. Nidogen 1 was thought to be central in the assembly processes, connecting the networks formed by collagen type IV and laminins, however, targeted inactivation of nidogen 1 resulted in no obvious phenotype. We have now selectively deleted the sequence coding for the 56 amino acid nidogen-binding site, γ1III4, within the *Lamc1* gene by gene targeting. Here, we show that mice homozygous for the deletion die immediately after birth, showing renal agenesis and impaired lung development. These developmental defects were attributed to locally restricted ruptures in the basement membrane of the elongating Wolffian duct and of alveolar sacculi. These data demonstrate that an interaction between two basement membrane proteins is required for early kidney morphogenesis in vivo.

Key words: Basement membrane, Wolffian duct, Kidney, Lung, Morphogenesis, Mouse

INTRODUCTION

Basement membranes are specialized extracellular matrices that play fundamental roles in tissue development and function. These thin sheet-like structures are produced through complex interactions between the major components laminins, collagen IV, the heparan sulfate proteoglycan perlecan and nidogen (Mayer and Timpl, 1993). Laminins are heterotrimeric cross-shaped multidomain molecules composed of three genetically distinct chains (α, β and γ). To date, 14 different laminin isoforms have been identified and the diversity is mainly due to the existence of five different α chains (Miner and Patton, 1999). Conversely, among the three known γ chains, the laminin γ1 chain shows a ubiquitous expression pattern and is found in all laminin isoforms, with the exception of laminin 5 and laminins 12-14 containing the γ2 and γ3 chain, respectively (Miner and Patton, 1999; Koch et al., 1999; Libby et al., 2000). Purification of laminin 1 under non-denaturing conditions demonstrated that nidogen 1 forms a stable complex with laminin (Paulsson et al., 1987). In addition, nidogen 1 has been shown to bind to most of the currently known basement membrane proteins, including perlecan and collagen IV (Timpl and Brown, 1996). The finding, however, that nidogen 1 can mediate the formation of ternary complexes between laminin and collagen IV in vitro (Fox et al., 1991), led to the hypothesis that it is crucial for basement membrane assembly, by connecting the major networks formed by laminins and collagen IV.

The precise mechanisms how basement membranes are assembled and how the biological function of the proteins is maintained within the basement membrane in vivo, are still unclear. In particular, the differential sites of synthesis for nidogen and laminin chains in mesenchymal and epithelial tissues, respectively, (Thomas and Dziadek, 1993; Ekblom et al., 1994) argues for the presence of other factors involved in the assembly processes. Recent results obtained by targeted deletion of cell-surface receptors, such as β1 integrins and dystroglycan showed disruption of basement membrane structures (Kreidberg et al., 1996; Williamson et al., 1997; DiPersio et al., 1997; Sasaki et al., 1998; Henry and Campbell, 1998) and emphasize a role for transmembrane complexes in coordinating the spatial and temporal local concentrations of proteins at the sites of basement membrane formation.

It is widely believed that basement membranes serve as both structural barriers and as a substrate for cellular interactions. The genetic inactivation of most of the major components has demonstrated that each of the proteins serves specific functions. Though all mutations interfere at specific stages with basement membrane integrity, the underlying mechanisms most probably differ. Mice deficient for perlecan develop normally before they die of heart failure at 10.5 day post coitum (dpc), because of basement membrane instability caused by mechanical stress

(Costell et al., 1999). Natural mutations within any of the laminin 5 chains (α3, β2, γ2) lead to junctional epidermolysis bullosa, a severe skin blistering disease (Pulkkinen and Uitto, 1999). Likewise, mutations within the laminin α2 chain result in congenital muscular dystrophies (Helbling-Leclerc et al., 1995). Targeted disruption of the laminin α5 chain is embryonic lethal because of local structural basement membranes defects at the site of expression of the corresponding laminin isoforms (Miner et al., 1998). None of these mutations, however, showed major early embryonic defects, reflecting the distinct expression of specific laminin isoforms and their function during embryonic development and adulthood. On the contrary, the crucial importance of laminins for basement membrane formation has been demonstrated by deleting 10 out of the 14 known laminin isoforms through the inactivation of the laminin γ1 chain. Mice, homozygous for the mutation lack basement membranes and die at 5.5 dpc through a failure of ectodermal and endodermal cell differentiation (Smyth et al., 1999; Murray and Edgar, 2000).

The nidogen-binding site of laminin has been localized to a single laminin-type epidermal growth factor-like (LE) module, γ1III4, of the laminin γ1 chain (Mayer et al., 1993b) and is therefore present in most of the laminin isoforms known. Though the γ2 chain of laminin 5 contains a highly homologous LE module, γ2III4, no significant binding activity has been observed (Mayer et al., 1995). LE motifs consist of about 60 amino acids and form four disulfide-bonded loops (Baumgartner et al., 1996; Stetefeld et al., 1996). Peptide and mutant analysis of the 56 amino acid nidogen-binding LE module demonstrated that two non-contiguous loops are necessary for high-affinity binding to nidogen 1 (Pöschl et al., 1994; Pöschl et al., 1996). Antibodies that inhibit the laminin-nidogen interaction perturbed epithelial branching morphogenesis in organ culture of lung, kidney and salivary glands, a process that involves formation of new basement membranes (Ekblom et al., 1994; Kadoya et al., 1997). Surprisingly, however, mice deficient for nidogen 1 failed to show any overt phenotype, which may be attributed to a redundancy of nidogen isoforms (Murshed et al., 2000).

In order to characterize the biological significance of the laminin-nidogen interaction, we have used a genetic approach to delete the nidogen-binding module γ1III4 of the laminin γ1 chain in the germline of mice, thereby abrogating binding of potentially redundant nidogen isoforms. The results show that while basement membrane formation is not crucially dependent on the laminin-nidogen interaction, there are structural abnormalities in specific basement membranes of kidney and lung, resulting in impairment of early kidney organogenesis and lung development.

MATERIALS AND METHODS

Construction of the targeting vector

A 164 bp cDNA fragment coding for γ1III4 was used for probing a lambda FIX II genomic library (Stratagene) of the mouse 129SvJ strain. Exons coding for domain III of the laminin γ1 chain were identified by hybridization with radiolabeled oligonucleotides according to the published human genomic organization of the *Lamc1* gene (Kallunki et al., 1991). The nidogen-binding module γ1III4 was contained within a 4.7 kb *Hin*dIII/*Bam*HI fragment. Deletion of γ1III4 was achieved within a unique 400 bp *Apa*I/*Nhe*I fragment using 5′-GATCGGGCCCGTGAGACTGTGCAAAGGTTAGTCACTGGCCAGACTCGGTCACG and 5′-ACAGAGATGTGCTAGCAATTAAAA-CACATTGCCC, and verified by sequencing. After subcloning the mutated *Apa*I/*Nhe*I fragment into the *Hin*dIII/*Bam*HI genomic clone, the HSV-TKNeo cassette flanked by two loxP sites was inserted into the *Nhe*I site in the following intron. To identify Cre recombination, an additional *Eco*RV restriction site was introduced after the second loxP site. The mutated clone was then extended by a 3′-following 5.2 kb *Bam*HI genomic fragment.

Generation of hetero- and homozygous ES cells

R1 cells were cultured and transfected with the *Not*I linearized targeting vector as described (Mayer et al., 1997). Genomic DNA from G418 resistant clones were screened by Southern hybridization after *Eco*RV restriction with a 0.5 kb *Hin*dIII/*Eco*RV fragment located upstream of the targeting vector. Positive clones were analyzed for additional random insertion using the neomycin gene as probe. Two clones were expanded and transiently transfected with Cre recombinase under the control of the PGK promoter. Deletion of the selection cassette was verified after *Eco*RV restriction using the same probe as described above. To obtain homozygous mutant ES cells, one of the positive clones was transfected once again with the initial targeting vector to obtain one allele still carrying the selection cassette (4.5 kb fragment) and one devoid of (2.7 kb).

Generation of mice lacking the nidogen-binding module γ1III4

Two independent heterozygous clones lacking the selection cassette, CIA2 and CIII3C6, were injected into C57/B6 blastocysts and transferred into pseudopregnant CD1 foster mothers. Highly chimeric male founder mice were obtained which were crossed with C57/B6 and 129Sv females to obtain heterozygous F_1 offspring. Heterozygous mice were mated to obtain time-staged homozygous embryos. All F_1 and F_2 progeny were genotyped by Southern blotting or by PCR using 5′-AGATGTGAACTCTGTGATGAC as forward and 5′-TGCAA-GAAGTGGTTCACACCGCATTCT as reverse primer.

Preparation of embryoid bodies

Undifferentiated ES cells were trypsinized, diluted in ES medium without LIF (EB medium) as described (Wobus et al., 1991) and plated onto cell culture dishes for 45 minutes to allow residual feeder cells to attach. The supernatant was washed twice with EB medium and ES cells were finally diluted at a concentration of 32×10^3/ml. The cells were then placed in hanging drops of 25 μl (Wobus et al., 1991). After 2 days, cell aggregates were transferred into EB medium filled bacterial dishes. Medium was changed every 48 hours. After 10 days in culture, intact embryoid bodies were collected, washed twice in PBS and further processed.

Protein analysis and rotary shadowing electron microscopy

Embryoid bodies were sequentially extracted with TBS and EDTA as described (Paulsson et al., 1987). The EDTA extract was passed over a Hi-Trap heparin affinity column (Pharmacia). Bound laminin was eluted with a linear NaCl gradient as previously described (Paulsson et al., 1987). Rotary shadowing electron microscopy was performed as described (Paulsson et al., 1987).

For radioimmuno inhibition assays (RIA) embryoid bodies from three independent homozygous mutant and control cells and embryos were extracted in RIPA buffer (Sasaki et al., 1996) and analyzed as described (Sasaki et al., 1998). For immunoblotting, 5 μg total protein were separated under non-reducing conditions on 5-15% SDS-PAGE gels, transferred onto PDVF membranes (Millipore) and incubated with the primary antibodies. Using goat-anti-rabbit antibodies conjugated with horseradish peroxidase (BioRad), specific bands were detected after visualizing enzyme activity with ECL (Amersham).

Northern blotting and RT-PCR

Total RNA was prepared using Trizol, according to the suppliers protocol (GibcoBRL). Samples (10 μg) of each genotype were electrophoresed in a 1.2% denaturing formaldehyde gel and transferred to HybondN membrane (Amersham) and hybridized against ^{32}P-oligolabeled cDNA probes for laminin γ1, laminin γ1III4, perlecan, nidogen 1 and nidogen 2. For standardization, the same membranes were reprobed with a GAPDH probe.

For RT-PCR, 5 μg of total RNA was reverse transcribed with MuLV reverse transcriptase (Appligene). For second strand synthesis 2 μl of the reaction mixture were used in PCR reactions. After 35 cycles, PCR products were analyzed on a 2% agarose gel. Control reactions were carried out without reverse transcription. Forward and reverse primers were chosen from different exons and were as follows: for demonstrating deletion of the nidogen-binding module γ1III4, 5′-AGATGTGAACTCTGTGATGAC and 5′-TTGTAGTAGCCAGGG-TCACAAGTA; for LE modules 6-7 of the laminin γ1III domain, located downstream of the deletion site, 5′-GTGTGACTGCC-ATGCTTTGGG and 5′-CTTCACAAGTCGGTAACAAGCCGG; for GAPDH, 5′-CTGCCAAGTATGATGACATCA and 5′-TACTCCTT-GGAGGCCATGTAG, yielding in reaction products of 369 and 201 bp for wild-type and mutated alleles for the deletion site, and 317 bp and 252 bp products for LE6-7 and GAPDH, respectively. The PCR products were verified by sequencing.

Histochemistry and immunohistochemistry

Embryos and tissues were dissected, fixed for 2-4 hours in 4% paraformaldehyde in PBS and either embedded in OCT or in paraffin wax. Paraffin wax-embedded sections (5-10 μm) were processed for Hematoxylin and Eosin staining.

For immunostaining 7-10 μm cryosections were stained with the respective antibodies. Paraffin wax-embedded sections were dewaxed and treated for 10 minutes with 100 μg/ml proteinase XXIV (Sigma) at 37°C. After a blocking step with PBS, 5% normal goat serum (NGS), first antibodies were applied in PBS, 2% NGS for 1 hour at 37°C in a humidified chamber. After washing with PBS, the sections were incubated with secondary Cy3- or Cy2-conjugated goat-anti-rabbit or goat-anti-rat antibodies. After final washing in PBS, sections were mounted and analyzed on an Axiophot fluorescence (Zeiss) and an Olympus confocal microscope. Primary antibodies used were rabbit antisera against nidogen 1 (Fox et al., 1991), nidogen 2 (Kohfeldt et al., 1998) and laminin 1, recognizing isoforms containing α1, β1 or γ1 chains (Fox et al., 1991), laminin γ1 recognizing the wild-type or the mutated protein (Mayer et al., 1998), perlecan, collagen IV (Costell et al., 1999), Pax2 (Babco), SP-C (Vorbroker et al., 1995) and rat anti-mouse monoclonal antibodies against nidogen 1 (Ries et al., 2001).

Electron microscopy

Tissue specimens (1 mm^2) were fixed in 3% paraformaldehyde and 3% glutaraldehyde in PBS for 2 hours at 4°C as described (Mayer et al., 1997). They were then postfixed for 1 hour in 1% osmium tetroxide and embedded in Epon. Ultrathin sections were collected on formvar coated copper grids, stained for 10 minutes with uranyl acetate, 5 minutes with lead citrate and examined with a Zeiss EM 109 electron microscope. For quantification of lung morphology, eight tissue samples of four homozygous mutant and four control mice were taken and a total of 200 randomly selected fields of 117 μm^2 counted for each genotype.

RESULTS

Targeted inactivation of the nidogen-binding site within the *Lamc1* gene abrogates nidogen binding

To explore the biological role of the laminin-nidogen interaction, a targeting vector was prepared that lacked the nidogen-binding LE module, γ1III4, within domain III of the laminin γ1 chain. The nidogen-binding module is encoded together with part of the preceding LE module in one exon. Deletion of γ1III4 was achieved using a PCR-based strategy, leaving 7 bp of the original sequence at the 3′-end of the exon, thus allowing fusion of γ1III3 directly to γ1III5 after splicing. The inserted selection cassette was flanked by two loxP sites and excised after transient transfection with Cre recombinase (Fig. 1A). Homologous recombination in embryonic stem cells (ES) was followed by the appearance of a 4.5 kb band for the targeted allele, which was further reduced in size to 2.7 kb after Cre-mediated recombination (Fig. 1B).

To analyze the role of the laminin-nidogen interaction in vitro, we generated ES cells homozygous mutant for the deletion (Fig. 1B). RT-PCR analysis with primers flanking γ1III4 showed the correct size of the amplified products for the wild-type and mutated alleles, indicating that the deletion close to the exon border did not interfere with transcription and correct splicing (Fig. 1C). To prove that the deletion of γ1III4 completely abolishes nidogen-binding activity, laminin was purified from wild-type and γ1III4-deficient embryoid bodies by heparin affinity chromatography. In agreement with earlier studies (Paulsson et al., 1987), nidogen 1 was retained together with laminin by the matrix in wild-type extracts, while it was exclusively detected in the flow through fraction in mutant extracts, demonstrating that mutant laminin had lost nidogen-binding activity (data not shown). This was further confirmed by rotary shadowing electron microscopy showing nidogen 1 closely associated with the short arm of laminin in controls, whereas a related structure was absent in the mutant laminin (Fig. 2). Furthermore, the typical cruciform shape and the correct number of globular domains in the short arms of the mutant laminin (Fig. 2) excluded the possibility that the deletion had interfered with folding and assembly of laminin into a trimer.

Embryoid bodies grown from wild-type and heterozygous cells did not show any overt differences compared with those devoid of the nidogen-binding site with respect to size and spontaneous contraction. Surprisingly, a clear basement membrane-like structure was identifiable below the outer endodermal layer in cross sections of mutant embryoid bodies by immunostaining (data not shown), indicating that the laminin-nidogen interaction is not a prerequisite for basement membrane formation, as suggested in earlier studies (Fox et al., 1991; Ekblom et al., 1994).

Kidney organogenesis is dependent on the laminin-nidogen interaction

Heterozygous mice derived from two independent ES cell lines were obtained and did not show any obvious phenotype up to one year of age. Immunostaining with antibodies specific for the interfaces of the tandem arrays of LE modules in the wild-type or mutant (Mayer et al., 1998) demonstrated that both the mutant and the wild-type laminin γ1 chain were present in basement membranes (data not shown). Genotyping of more than 800 offspring of heterozygous crossings at weaning failed to reveal any surviving homozygous mutant animals (+/+:+/–:–/–; 280:524:0). Dead pups were routinely observed shortly after birth of which most were homozygous for the mutation. This suggested that mice deficient for the nidogen-binding module γ1III4 died soon after birth. However, phenotype analysis during prenatal development showed that

only ~60% of the mutant embryos developed to term, whereas ~40% died before 11.5 dpc for so far unknown reasons.

Embryos were removed at 18.5 dpc by Caesarian section. The majority of the mutant embryos were about 20% smaller than their littermate controls. Strikingly, visual inspection demonstrated the lack of kidneys in most homozygous embryos (Fig. 3C,E) whereas they were present in all wild-type (Fig. 3A,D) and heterozygous embryos analyzed. Both kidneys were identifiable in only a small percentage of mutant embryos (Fig. 3B), while ~90% showed either bilateral (80%; 46 out of 59 animals) or unilateral (10%; 5 out of 59 animals) renal agenesis, demonstrating that the laminin-nidogen interaction plays a pivotal role during kidney organogenesis. The low penetrance of metanephric development was independent of the ES clone or genetic background being observed on a heterogeneous (C57/129Sv) as well as on a 129Sv background. Despite the lack of kidneys, adrenal glands, testis and ovary were normally present with gross and histological analysis failing to reveal any abnormalities in these organs, while the uterus in female and vas deferens and the seminal vesicles in male mutants were absent (Fig. 3C,E).

Growth of Wolffian duct is impaired in γ1III4-deficient mice

An essential step during kidney development involves growth of the Wolffian duct and its subsequent fusion with the cloaca, a prerequisite for the outgrowth of the ureteric bud (Saxen et al., 1987). The ureteric bud subsequently induces the metanephric mesenchyme to condense and to undergo a mesenchymal-epithelial conversion. As kidney organ culture studies have demonstrated that less new epithelium formed around the tips of the ureteric bud in the presence of antibodies inhibiting the laminin-nidogen interaction (Ekblom et al., 1994), defective epithelialization could have led to subsequent degeneration of the kidney anlage, resulting in renal agenesis. We therefore analyzed kidney development at 13.5 dpc with standard histological techniques. In all wild-type and heterozygous embryos, multiple branches of the ureteric bud surrounded by condensed metanephric mesenchyme were observed (Fig. 4A) that were indistinguishable in number and

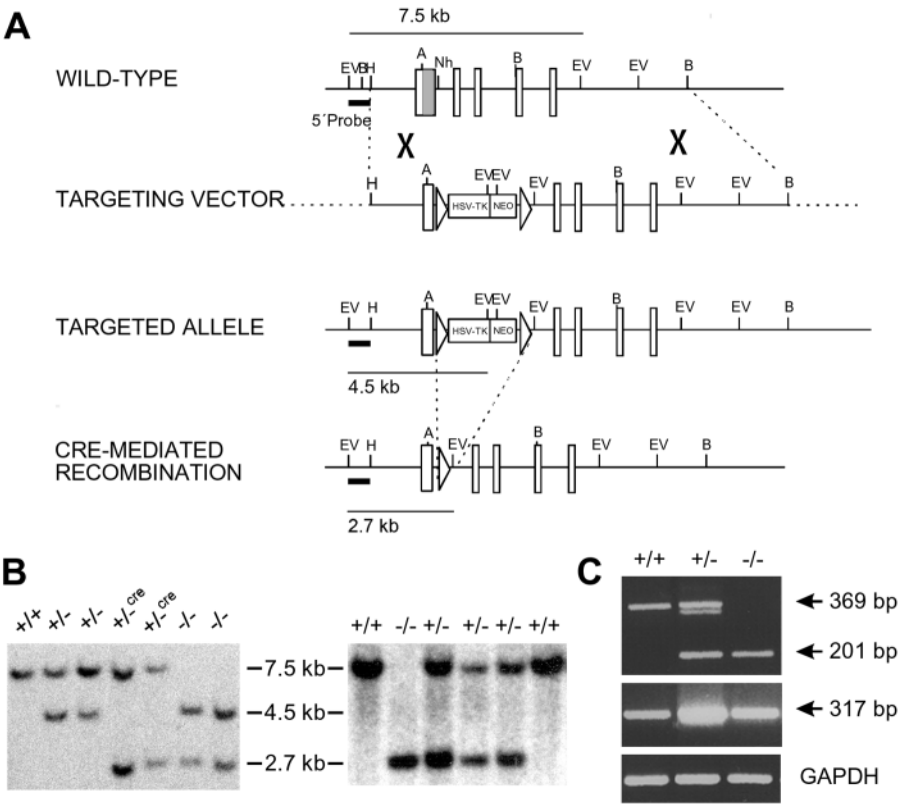

Fig. 1. Generation and analysis of ES cells and mice lacking the nidogen-binding module γ1III4. (A) Restriction map for the genomic region of domain III of the *Lamc1* gene. The sequence coding for the nidogen-binding module γ1III4 is depicted in gray. The targeting vector and the resulting targeted allele after homologous recombination in ES cells are shown below. The final targeted allele was achieved by Cre-mediated deletion of the selection cassette. Predicted sizes of genomic fragments after *Eco*RV restriction and Southern blotting, using the externally located 5′ probe, are indicated. A, *Apa*I; B, *Bam*HI; EV, *Eco*RV; H, *Hin*dIII; Nh, *Nhe*I. (B) Southern blot analysis of *Eco*RV digests of genomic DNA from respective ES cell clones (left panel) and F_2 embryos at 18.5 dpc (right panel). A fragment of 7.5 kb is detected in the wild type. In addition, a 4.5 kb fragment is seen in heterozygous cells, which is further reduced in size to 2.7 kb after transient transfection with Cre (+/–^{cre}). Homozygous mutant embryos were identified by the appearance of a single 2.7 kb band (right panel), whereas homozygous ES cells showed both a 4.5 and a 2.7 kb band (left panel). (C) RT-PCR analysis of RNA isolated from wild-type (+/+), heterozygous (+/–) and homozygous mutant (–/–) ES cells. Primer pairs spanning the deletion site resulted in the expected size of fragments for the wild-type (369 bp) and mutated (201 bp) laminin γ1 chain (top panel). In all genotypes, the downstream located modules γ1III6-7 (middle panel) are normally transcribed.

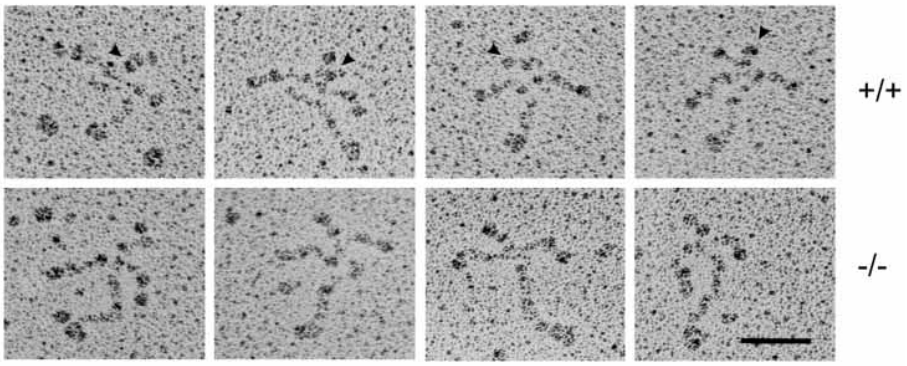

Fig. 2. Rotary shadowing electron microscopy demonstrates the absence of nidogen in homozygous mutant (–/–) laminin compared with the wild-type (+/+) form (arrowheads). Scale bar: 50 nm.

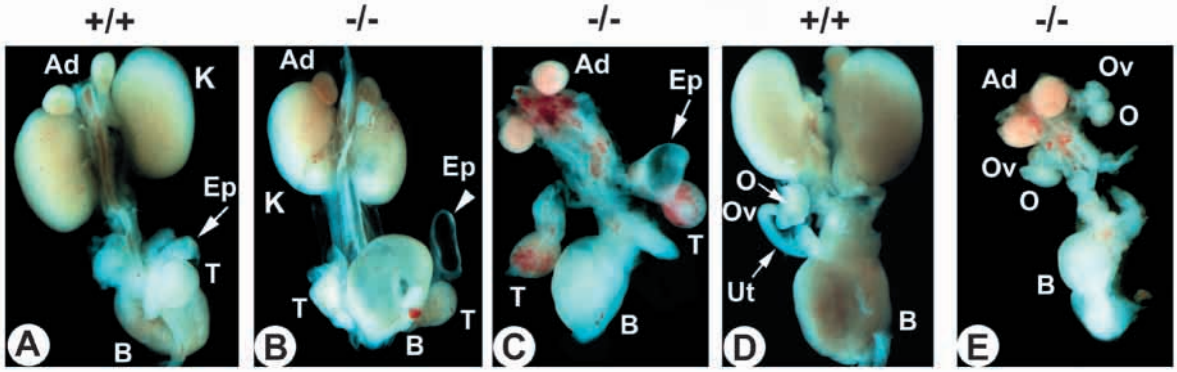

Fig. 3. Bilateral renal agenesis in laminin γ1III4-deficient mice. Urogenital tracts were dissected from male (A-C) and female (D,E) embryos at 18.5 dpc. Eighty percent of the homozygotes display bilateral renal agenesis (C,E). Testis (C) and ovary (E) are normally present, but ureter, vas deferens and uterus are lacking. Ten percent of the homozygous mutant animals develop two kidneys (B). The remaining of the urogenital system appears normal, except the epididymis, which has a vesicular appearance (arrowhead in B). Ad, adrenal gland; B, bladder; Ep, epididymis; K, kidney; O, ovary; Ov, oviduct; Ut; uterus; T, testis.

morphology from those mutant embryos in which either one or two metanephric kidneys had been induced (Fig. 4C). However, in the majority of γ1III4-deficient embryos, only remnants of uncondensed metanephric blastema were observed (Fig. 4B).

This raised the possibilities that either the ureteric bud failed to branch from the Wolffian duct at earlier stages or that its growth towards the metanephric mesenchyme was defective. At 11 dpc, the first dichotomous branching of the ureteric bud was visible in all wild-type, heterozygous and a few mutant embryos (Fig. 4D,F). In most of the mutant embryos, however, we were not able to identify any signs of the ureteric bud (Fig. 4E) and thus defective or delayed growth followed by cell death could be excluded. Surprisingly, a morphologically identifiable Wolffian duct was also absent in the caudal region of the embryos. During embryonic development, two pairs of renal organs, the pronephros and the mesonephros, are formed in a spatial and temporal sequence before the metanephros becomes the adult functional kidney. As all three organs are formed by mesenchymal-epithelial transition, kidney agenesis could have been explained by a general failure of this conversion. Yet, the mesonephros was properly formed and in size and number of tubuli similar to wild-type embryos at 11.5 dpc (Fig. 5A,B). At the same stage the caudal progression of the Wolffian duct towards the cloaca could be followed in serial sagittal and tranverse sections in wild-type embryos (Fig. 5C). In eighteen γ1III4-deficient embryos devoid of metanephric kidney induction, however, the Wolffian duct was blind-ending within the upper level of the urogenital ridge (Fig. 5D). In support of these data, at 13.5 dpc we also observed a blind-ending Müllerian duct, which is known to develop in parallel to and to be dependent on an inductive influence of the Wolffian duct (Jacob et al., 1999). Despite the absence of a ureteric bud, we could identify distinct uninduced metanephric mesenchyme in all cases.

Growth of the Wolffian duct is still poorly understood. We speculated that a defective basement membrane along the duct might cause retardation of its growth. Yet, immunostaining for laminin revealed normal, linear basement membrane structures (Fig. 5F). A closer inspection by confocal microscopy, however, demonstrated that discontinuities close to the growing tip of the Wolffian duct existed in deeper layers of the sections, and that the normally tightly connected epithelial cells were partially separated (Fig. 5G). These results

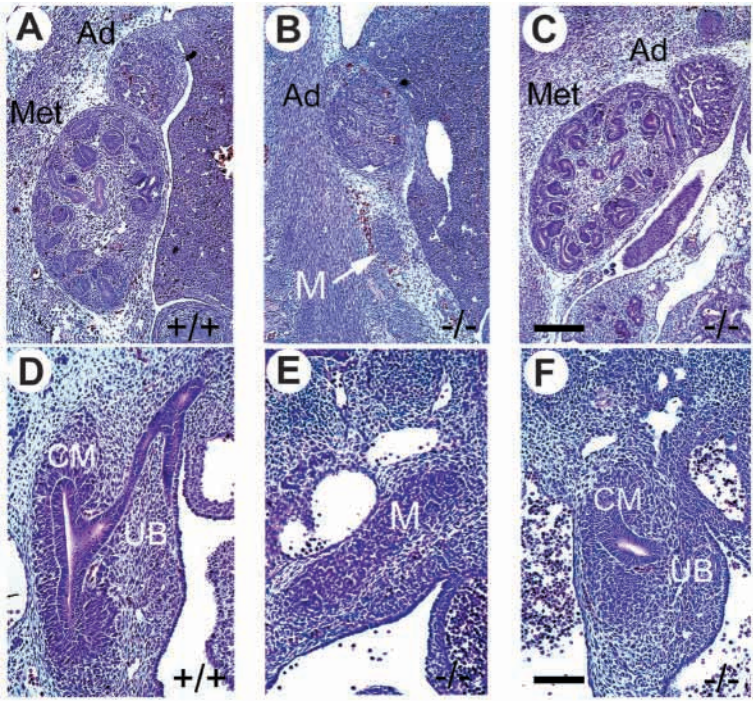

Fig. 4. Metanephric kidney development in 13.5 and 11.5 dpc embryos. Morphology of representative sagittal H&E stained sections of 13.5 (A-C) and 11.5 dpc (D-E) embryos. At 13.5 dpc, the metanephric kidney is well developed in wild-type embryos (A) and a few homozygous mutant embryos (C). In the majority of mutant embryos, the metanephros is lacking and only remnants of the metanephric mesenchyme (arrow) are visible (B). At 11.5 dpc, the ureteric bud has invaded the mesenchyme and bifurcated once, surrounded by condensed metanephric mesenchyme in wild-type (D) and a few mutant embryos (F). In the majority of mutant animals, only uninduced metanephric mesenchyme is present (E). Ad, adrenal gland; CM, condensed metanephric mesenchyme; M, metanephric mesenchyme; Met, metanephric kidney; UB, ureteric bud. Scale bars: 150 μm in A-C; 50 μm in D-F.

were further supported by electron microscopy showing that basement membranes were interrupted by gaps along the Wolffian duct (see Fig. 9D,E). Epithelial cell shape and polarity, however, appeared normal. To determine whether growth retardation is correlated with a decrease in cell proliferation, we performed BrdU-labeling in utero and found that the number of BrdU-positive cells was not significantly changed compared with controls (Fig. 5G). Similarly, staining for Pax2, a transcriptional regulator of the paired-box family known to result in Wolffian duct dysgenesis (Torres et al., 1995) was normal (Fig. 5H,I). From these data, we conclude that growth inhibition of the Wolffian duct in γ1III4-deficient embryos is dependent on a locally restricted defective basement membrane, but independent of a proliferation defect or differentiation processes regulated by Pax2.

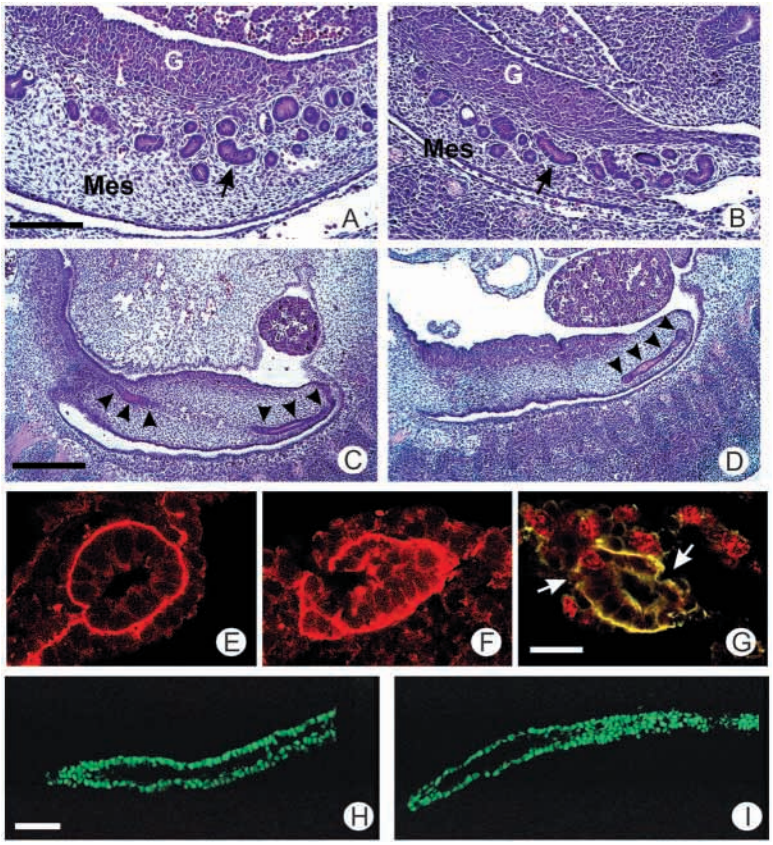

Fig. 5. Wolffian duct in 11 dpc embryos. The mesonephric kidney is comparably developed in γ1III4-deficient (B) and in wild-type (A) embryos (arrows). (C,D) Growth of the Wolffian duct (arrowheads) can be followed in consecutive sagittal sections throughout the urogenital ridge in wild-type (C) but not in mutant (D) embryos. A representative sections of the blind-ending Wolffian duct in mutant embryos is shown in D. Confocal microscopy after immunostaining for laminin (E-G) and BrdU (red label in G) reveals continuous basement membranes structures in the controls (E) and mutants (F), which are, however, partially interrupted (arrows) in deeper layers of the section (G). Pax2 (H,I) is normally present in the Wolffian duct in the mutants (I) compared with littermate control embryos (H). Scale bars: 100 μm in A,B; 250 μm in C,D; 40 μm in E-G; 50 μm in H,I.

Kidney dysgenesis caused by the absence of the laminin-nidogen 1 interaction

Kidney agenesis occurred in 90% of the animals. In the 10% of mutant embryos in which kidney development did occur, we observed normal kidney architecture with multiple branches of the ureteric bud between 11.5 and 13.5 dpc (Fig. 4C,F). At 18.5 dpc, however, mutant kidneys seemed to be non-functional, as the urinary bladders were morphologically empty. Dysgenesis of variable severity was apparent in the mutant kidneys. While the outer developing cortical region was comparable with the control tissues, the quantity of tubular structures in the mature region was greatly diminished (Fig. 6A,B). Furthermore, histological sections revealed abnormalities in the glomeruli of the inner cortical region. The total number of mature glomeruli counted in kidney sections obtained from three individual animals was 30% less than in wild-type kidneys. Of these, 60% were normally developed (Fig. 6C), whereas the rest had either a reduced (25%) or missing (15%) capillary tuft, and consequently the Bowman's capsule was partially or completely filled with red blood cells (Fig. 6D,E). The distal and proximal tubuli, as well as all Comma- and S-shaped bodies were surrounded by an ultrastructurally distinct basement membrane. The same was found for the majority of glomerular basement membranes (GBM), although when the capillary tuft was missing the GBM was not linear but interrupted (data not shown).

In addition, some of the mutant kidneys analyzed showed cystic enlargements, which were only observed in male homozygotes. To define the defect more closely, we followed the ureter in transverse sections from three male mutant embryos at 18.5 dpc caudally towards the bladder. A hydronephric kidney with a thinned parenchyma was apparent (Fig. 6F) and the ureter connected aberrantly either to the vas deferens (Fig. 6G) or, in one case, ended directly in the epididymis, both derivatives of the Wolffian duct. During dissection of the urogenital tracts, we observed a vesicular structure in close vicinity to the testis in mutant embryos (Fig. 3B), which was identified as epididymis. These data therefore strongly suggest that in these males, the kidney directly drained into the genital tracts, thus leading to loss of the normal architecture of the epididymis.

Nidogen 1 is not retained in basement membrane structures

To determine whether the deletion of γ1III4 within the laminin γ1 chain affects the localization of nidogen, we performed immunostaining of various tissues. Nidogen 1 was present in all basement membranes of wild-type and heterozygous animals, but, with a few exceptions, barley detectable in basement membrane structures of the mutant animals. Only basement membranes around large blood vessels and at the dermal-epidermal junction of the skin showed staining intensities comparable with the control tissues (data not shown). This raised the question as to whether the recently newly identified, highly homologous isoform, nidogen 2 (Kohfeldt et al., 1998), is upregulated. Double-immunostaining for nidogen 1 and nidogen 2 in kidney sections, however, indicated that nidogen 2 was neither differently deposited nor

was its staining intensity increased relative to the controls (Fig. 7A-D). Staining intensities similar to that of wild-type controls were also observed for the laminin γ1 chain (Fig. 7E,F), collagen IV and perlecan (data not shown).

Former studies have demonstrated that nidogen 1 is highly susceptible to proteases and that complex formation with laminin protected the C-terminal globular domain G3 from degradation (Mayer et al., 1993a). Surprisingly, immunoblotting of various tissue extracts showed normal levels of non-degraded nidogen 1 (Fig. 7G), excluding the possibility that nidogen 1 is lost due to excessive proteolysis. Comparable RNA and protein levels for nidogen 1, nidogen 2, laminin and perlecan were also found by radioimmuno inhibition assays and Northern blotting (data not shown). We therefore conclude that through the deletion of the nidogen-binding site, no compensatory mechanisms are induced, but that nidogen 1 is lost during embedding procedures, thus strongly arguing for a weakened integration into basement membranes caused by the deletion of its binding site.

Lung defects might cause perinatal lethality in γ1III4-deficient mice

Homozygous mice die very soon after birth and, despite the fact that the kidney phenotype should lead to a perinatal lethality within the first 2 days, we have been unable to identify any living offspring within the first postnatal day. This indicated that another defect causes death of the homozygous animals. Indeed, some of the mutant dead pups had a cyanotic appearance indicative of respiratory problems.

Mutant lungs dissected from 18.5 dpc embryos, were normally developed with respect to number of lobes. Cross-sectioning through the lung revealed that the major bronchial trees had formed in the homozygotes, but they were more compact and smaller compared with wild type (Fig. 8A,B). At higher magnification, it became apparent that the prealveolar sacculi were immature and only poorly inflated, and mesenchymal thickening between the terminal airspaces was observed (Fig. 8C,D). Interaction between mesenchyme and epithelium is a crucial factor throughout lung development. Yet, between 11.5 and 13.5 dpc, no differences in number of buds or sizes of the lungs were observed compared with control embryos (Fig. 8E,F). The presence of surfactant protein C (SP-C) positive cells in 18.5 dpc mutant lungs further indicated that differentiation of precursor epithelial airway cells had proceeded (Fig. 8G,H).

Formation of the thin air-blood barrier is a crucial event for gas exchange and hence crucial for survival. Ultrastructural analysis of four individual γ1III4-deficient embryos at 18.5 dpc demonstrated that only ~10% of the prealveolar sacculi had formed, when compared with controls. In addition, when the air-blood barrier of the homozygotes had formed, the basement membranes showed severe abnormalities, while in the wild type, endothelial and epithelial cells were separated by a fused basement membrane (Fig. 9A-C). The alveolar basement membranes were apparently normal in 30% of the mutants (Fig. 9B), whereas only amorphously deposited material was detected in a further 30% (Fig. 9C). Remarkably, in the remaining alveoli, basement membranes were completely missing and epithelial cell protrusions were seen entering into the empty space (Fig. 9B). Together, these data suggest that the laminin-nidogen interaction is crucially important for the formation of the air-blood interface. Insufficient gas exchange, therefore, may have resulted in perinatal death of the mutant animals.

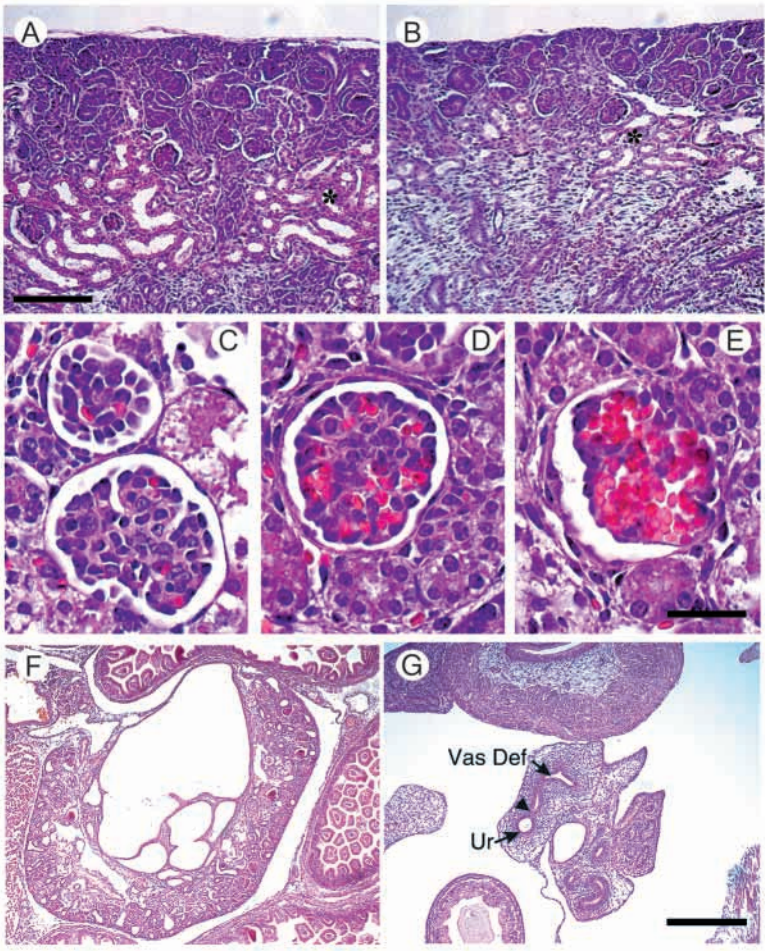

Fig. 6. Kidney abnormalities in 18.5 dpc embryos that are associated with the mutation. The outer cortical layer in the mutant embryos (B) is indistinguishable from the controls (A). Note, however, the reduced number of tubuli (asterisk) in the mutants (B). (C-E) Glomerular defects in the mutants are visible in the inner cortex with the glomerular tufts showing mild (D) to severe (E) capillary aneurysms compared with normal appearance (C). Mutant male embryos display a hydronephric kidney with a thin kidney parenchyma (F). (G) Consecutive transverse section of the same animal as shown in F, demonstrating fusion (arrowhead) of the ureter with the vas deferens. Ur, ureter; Vas Def, vas deferens. Scale bars: 100 μm in A,B; 25 μm in C-E; 250 μm in F,G.

DISCUSSION

The laminin-nidogen interaction is not a prerequisite for basement membrane formation

During embryonic development, laminin 1 and nidogen 1 are first expressed at the four- and 32-cell stages, respectively

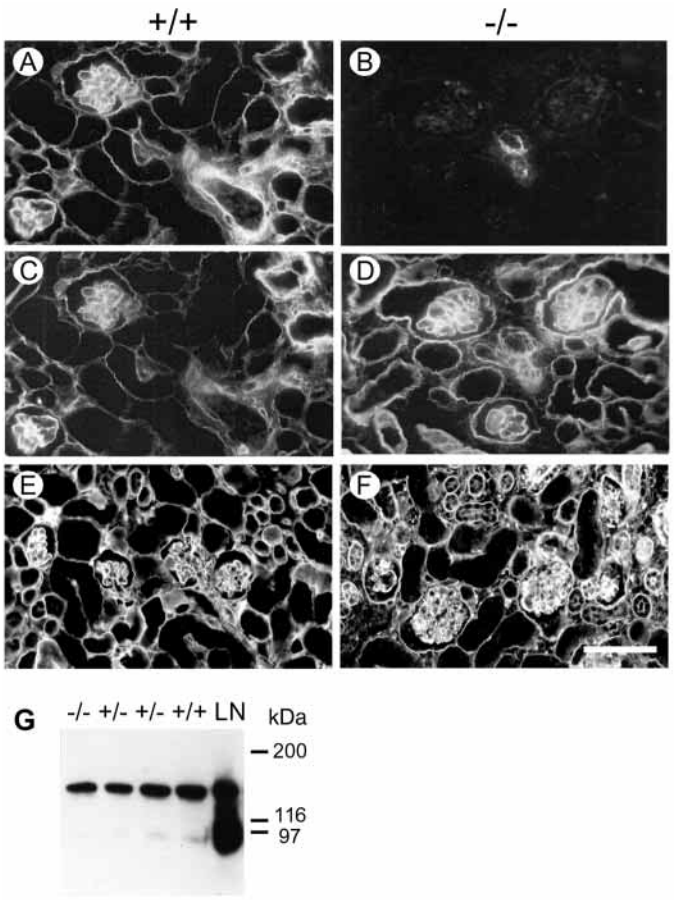

Fig. 7. Analysis of basement membrane components in 18.5 dpc tissues. Double-label immunofluorescence analysis (A-D) of nidogen 1 (A,B) and nidogen 2 (C,D) in kidney sections demonstrates strongly reduced levels of nidogen 1 immunoreactivity in the mutants (B), whereas nidogen 2 (D) is normally present. (E,F) Localization of the laminin γ1 chain to basement membrane structures is unaffected through the mutation (F) compared with controls (E). (G) Immunoblot analysis of extracts prepared from lung tissues shows comparable amounts of intact nidogen 1 in mutant lysates. LN, purified laminin-nidogen complex as control. Scale bar: 50 μm in A-F.

(Dziadek and Timpl, 1985). Although two additional γ chains (γ2, γ3) have been identified, the nidogen-binding γ1 chain is present in 10 out of 14 known laminin isoforms and in all basement membranes. Furthermore, deletion of the γ1 chain in mice resulted in early embryonic lethality (Smyth et al., 1999), but did not allow the determination of the function of the laminin-nidogen interaction. The potential of nidogen 1 to bridge the laminin and collagen IV networks (Fox et al., 1991) and the impaired branching morphogenesis in kidney and lung organ cultures in the presence of antibodies that interfere with the laminin-nidogen interaction (Ekblom et al., 1994; Kadoya et al., 1997), have led to the proposal that the laminin-nidogen interaction is involved in orchestrating the basement membrane assembly process.

The poor retention of nidogen 1 in the majority of basement membrane structures of γ1III4-deficient tissues was not expected, although the protein level determined was normal. Nidogen 1 has a highly versatile binding repertoire for other basement membrane components (Timpl and Brown, 1996), including a high-affinity interaction to the perlecan core protein (Hopf et al., 1999). The finding that normal immunoreactivity was only apparent in a few basement membrane structures, strongly argues that nidogen 1 is preferably integrated into basement membranes via laminins containing the γ1 chain.

It has previously been shown that inactivation of the *Nid1* gene in mice and *C. elegans* did not interfere with basement membrane formation and the animals are viable and were fertile (Murshed et al., 2000; Kang and Kramer, 2000). Yet, compensation by nidogen 2, which has a highly homologous domain structure and binding repertoire (Kohfeldt et al., 1998), might be the reason for the lack of phenotype in *Nid1* mutant mice (Murshed et al., 2000), and, vice versa, the same may be true for mice with a mutation in *Nid2* (Mitchell et al., 2001). Although human nidogen 2 binds with only low affinity to the nidogen 1-binding site within the laminin γ1 chain (Kohfeldt et al., 1998), the murine homolog has now been shown to be similar in binding affinity as nidogen 1 (T. Sasaki and R. Timpl, personal communication). It will therefore be of interest to see whether the double mutation of both genes reflects the phenotype described here for the deletion of the nidogen-binding site. Together, the genetic analyses supports the conclusion that neither nidogen 1 (Murshed et al., 2000; Kang and Kramer, 2000) nor, as shown here, its binding site on the laminin γ1 chain are crucial for basement membrane assembly and function in most tissues. Only a few tissues, including the cortex and neural tube, showed subtle discontinuities in basement membranes and developmental abnormalities (Halfter et al., 2002), arguing for a specific physiological function of the laminin-nidogen interaction. However, we cannot exclude the possibility that other, presently unknown functions of the nidogen-binding module of the laminin γ1 chain might contribute to the described phenotype.

The laminin-nidogen interaction is crucially important for Wolffian duct growth

Genetic data obtained from human diseases and transgenic mice have implicated transcription and growth factors, cell-surface receptors and extracellular matrix components in metanephric development (Lechner and Dressler, 1997; Müller and Brändli, 1999). Renal agenesis to a variable degree was manifested by mutations in several of these genes. Perturbed communication between cellular receptors and their respective ligands on either the metanephric blastema or the ureteric bud have been suggested in null-mutations for the glial cell line-derived neurotrophic factor, GDNF, and the tyrosine kinase receptor Ret (Lechner and Dressler, 1997), as well as in integrin α8-deficient mice (Müller et al., 1997), leading to defective metanephric kidney induction. However, renal agenesis in the absence of the laminin-nidogen 1 interaction is due to defects in Wolffian duct elongation and therefore manifests earlier during development.

The Wolffian duct develops from the intermediate mesoderm and gives rise to parts of the male genital system. In agreement with a primary defect in Wolffian duct growth, vas deferens and the seminal vesicles in male mutant embryos were missing, while the testes were normally present. The female genital tracts originate from the Müllerian duct, which forms later in development in parallel to the Wolffian duct, and its growth was shown to be dependent on an inductive influence of the

former (Jacob et al., 1999). In support of these data, we found both ducts to be blind-ending in the urogenital ridge in 13.5 dpc embryos and the female mutants to lack the uterus and occasionally the oviduct.

The Wolffian duct develops in the absence of the laminin-nidogen interaction, excluding its contribution to the first mesenchymal-to-epithelial transition that occurs in kidney development (Saxen, 1987), but its growth caudally towards the cloaca is inhibited. A similar phenotype was described for the targeted ablation of Pax2, a member of the paired-box family of regulatory transcription factors. As γ1III4-deficient mice, *Pax2* mutants fail to form parts of the genital tract and the ureteric bud (Torres et al., 1995), suggesting that growth of the Wolffian duct is affected in a similar manner. One possibility therefore is that deletion of the nidogen-binding site interferes with Pax2 expression in the epithelial tube. Yet, normal immunostaining of Pax2 in the mutant Wolffian duct indicates that it is not affected through the deletion.

Although we do not know the detailed mechanism responsible for the phenotype of our γ1III4 mutants, these mice now provide a model system to further our understanding of Wolffian duct growth and elongation, which has long been a subject of interest because of its central position in urogenital development. Once formed, the duct progressively elongates; so far two mechanisms have been proposed for this process: one suggests autonomous growth through cell proliferation at the tip of the duct, whereas a second model proposes that mesenchymal cells are continuously added by an epithelial transition (Saxen, 1987). The data presented here provide evidence that Wolffian duct elongation through autonomous cell proliferation at its growing tip can be excluded. First of all, the number of BrdU-positive cells were similar in mice with the nidogen-binding site deletion as in controls, and did not accumulate at the tip of the growing duct, but uniformly spread over the length of the duct as it has been described in amphibians (Overton, 1959), indicating that the underlying mechanisms are not due to reduced cell proliferation. Strikingly, however, we identified subtle local ruptures in the basement membrane close to the tip of the duct that may well interfere with duct elongation. Nidogen-binding to laminin could modulate the conformation of laminin or affect the spatial relationships between basement membrane components, which facilitate their interaction with cellular receptors. We therefore propose that the locally restricted discontinuities seen in basement membranes around the Wolffian duct are due to a perturbed cell-matrix interaction, which in turn interferes with signaling cascades necessary to induce the genetic program to recruit mesenchymal cells.

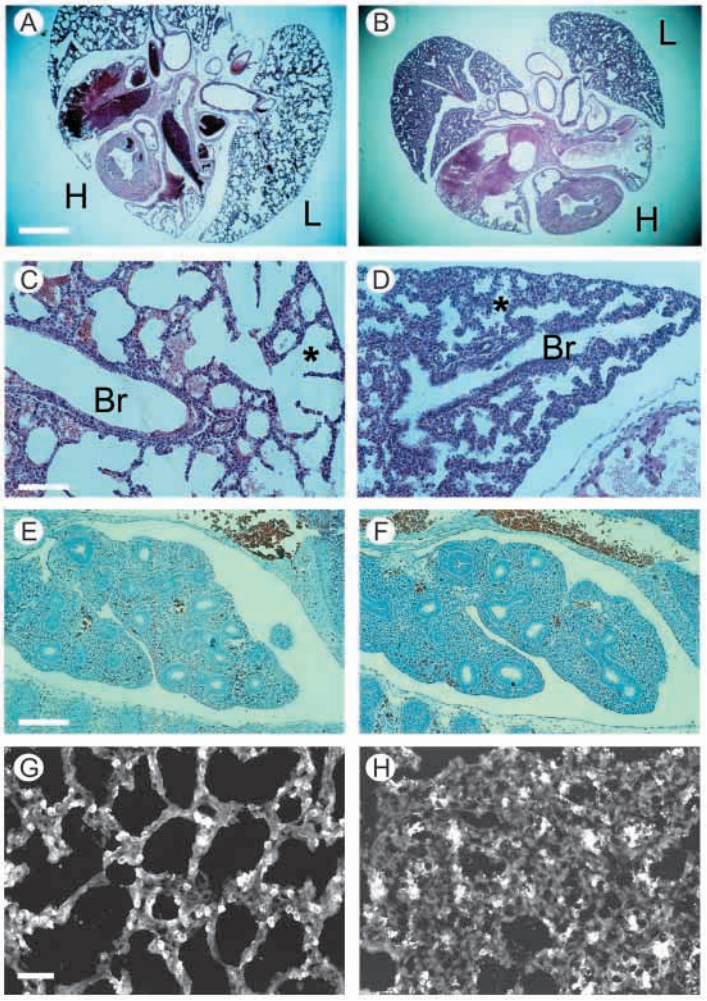

Fig. 8. Histology of lung tissue from γ1III4-deficient embryos. Representative sections of the lungs of mutant (B,D,F,H) and control (A,C,E,G) embryos through comparable regions are shown. Note the smaller and more compact size of the mutant lung (B) compared with controls (A) at 18.5 dpc. At higher magnification, it is apparent that the alveoli (asterisk) in γ1III4-deficient embryos (D) are only poorly developed with marked mesenchymal thickening around the terminal air spaces compared with wild type (C). At 13.5 dpc, no apparent differences in lung development are visible in mutant (F) when compared with wild-type (E) embryos. Staining for surfactant protein C demonstrates that differentiation of airway epithelial precursor cells is not defective (G,H). Br, Bronchiole; H, heart; L, lung. Scale bars: 1 mm in A,B; 250 μm in C,D; 100 μm in E,F; 50 μm in G,H.

The function of the laminin-nidogen interaction for epithelial branching morphogenesis in kidney and lung

The laminin-nidogen interaction has been suggested to be crucial for epithelial branching morphogenesis in general (Ekblom et al., 1994; Kadoya et al., 1997). Our data indicate that early branching morphogenesis of the lung is not disturbed in the absence of the laminin-nidogen interaction. However, shortly before birth, the lungs were only poorly inflated, with a mesenchymal thickening of the distal airspaces. Consequently, a respiratory problem caused with high probability the death of all the mutant pups. Interestingly, a similar phenotype has been reported in the absence of TGFβ3 (Kaartinen et al., 1995). The phenotype in TGFβ3-deficient mice has been correlated with reduced number of airway precursor cells (Shi et al., 1999). Although we identified these cells in γ1III4-deficient lungs by staining for SP-C, a detailed statistical analysis at different developmental stages is required to determine whether they are formed in similar numbers as in wild type. Ultrastructural analysis demonstrated that the majority of the distal airspaces in the mutants were uninflated,

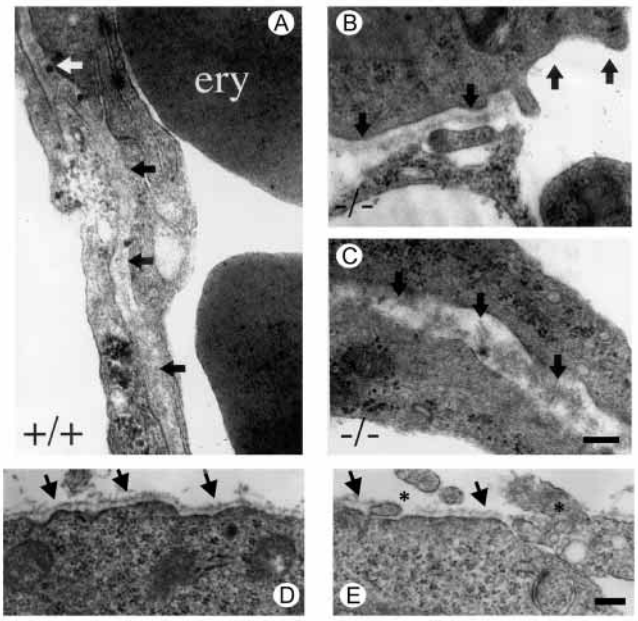

Fig. 9. Ultrastructural analysis of the elongating Wolffian duct and lung. Ultrastructural analysis demonstrates a well-developed basement membrane separating the air-blood space of the alveoli (arrows) in control tissue (A) at 18.5 dpc. In the mutant lungs, normal (B), amorphously deposited (C) and missing (B) basement membranes are present (arrows). Note the cell protrusion when basement membranes are missing (B). At 10.5 dpc, basement membranes of the elongating Wolffian duct show discontinuities (asterisk) next to normal electron dense structures (arrows) in the mutant (E) when compared with controls (D). ery, erythrocyte. Scale bars: 100 nm in A-C; 50 nm in D,E.

disorganized structures containing epithelial and mesenchymal cells. Strikingly, those sacculi that had formed the alveolar basement membranes showed severe abnormalities, being either amorphously deposited or absent. There are several potential explanations for this finding. A perturbed laminin-nidogen interaction could result in a differentiation deficit of airway precursor cells into type II and type I alveolar pneumocytes, or, alternatively, might interfere with their polarization. Cell contact with basement membranes has been suggested to be regulatory for sorting proteins to the apical or basolateral surfaces (Rodriguez-Boulan and Nelson, 1989). A possible scenario could therefore be that in the mutants, cell-surface receptors are wrongly translocated to the apical surface, and subsequently basement membrane assembly and formation of the air-blood barrier cannot take place. Further studies with in vitro lung organ cultures will be needed to distinguish between these possibilities.

Stochastic events are most likely to be behind observations that a proportion of mice with inactivated genes can to some extent overcome developmental problems. For example, deficiencies for the integrin $\alpha 4$ and α_v subunits or perlecan, have independent lethal phenotypes at different developmental stages, depending on the individual animal (Yang et al., 1995; Bader et al., 1998; Costell et al., 1999). Furthermore, variable penetrance of impaired kidney development has been observed upon mutations of the integrin $\alpha 8$ subunit, Ret or GDNF (Schuchardt et al., 1996; Moore et al., 1996; Müller et al., 1997). Similarly, a minority of the γ1III4-deficient animals displayed metanephric development, which may be due to either intact or regenerated basement membranes along the Wolffian duct at crucial stages of development. However, the number of tubuli and glomeruli in the mature part of the cortex in 18.5 dpc mutant kidneys was reduced even in those mutants in which induction of the metanephric blastema and branching of the ureteric bud proceeded without any obvious defects. Inhibition of the laminin-nidogen interaction by antibodies led to reduced tubulogenesis in an in vitro organ culture model, although in contrast to the present observations in vivo, basement membranes were largely distorted in the in vitro analysis (Ekblom et al., 1994). Thus, although the basement membrane architecture in the γ1III4-deficient kidneys appeared normal, it is tempting to speculate that locally restricted and transient basement membrane ruptures also occur during kidney morphogenesis, resulting in the differentiation defect.

Unexpectedly, the bladder of the mutant animals was empty even when kidneys had developed. The histological analysis in male mice demonstrated that the ureter failed to open into the bladder but instead stayed connected aberrantly either to the vas deferens or the epididymis, both derivatives of the Wolffian duct. The cysts seen in these kidneys are therefore likely to be secondary to a defect in urine outflow. These results also indicate that the reduction of the glomerular tufts is attributed to increased pressure through a tailback of the urine, rather than by a primary defect in mesangial cells as described in *Pdgfb* mutant mice (Leveen et al., 1994), and their GBM may rupture because of mechanical stress. Interestingly, this phenotype resembles congenital anomalies of the kidney and urinary tract (CAKUT) found in humans and mice (Pope et al., 1999). An abnormal ureter connection in conjunction with a hydronephric kidney has been reported for heterozygous Bmp4 mutant mice (Miyazaki et al., 2000). In these mice it is suggested that a deficit in BMP4 levels inhibits branching of the ureterovesicle junction into the cloaca as a result of impaired elongation of the ureter (Miyazaki et al., 2000). This model is reminiscent to the growth defect of the Wolffian duct in the urogenital ridge in the γ1III4 mutant animals. We therefore propose that a similar mechanism to that described above leads to the aberrant ureter fusion. However, we cannot exclude at the moment that the absence of the laminin-nidogen interaction causes subtle changes in the supramolecular organization of basement membranes, which then in turn could interfere with the sequestration of BMP4 or other growth and morphogenetic factors, or that specific unknown physiological functions exist for the nidogen-binding module, γ1III4 of the laminin γ1 chain

The authors thank Drs J. W. Fox, J. A. Whitsett and K. Rajewsky for their generous gifts of antibodies and selection cassettes; Dr A. Nagy for providing R1 embryonic stem cells; and H. Wiedemann for rotary shadowing electron microscopy. We gratefully acknowledge the excellent technical assistance by H. Alberty-Hornberger, V. van Delden and M. Reiter, and thank Dr D. Edgar for critical reading the manuscript and helpful discussion. N. S. is funded by the Bundesministerium für Bildung und Forschung in the framework of the Centre for Molecular Medicine Cologne. This work was supported by the Deutsche Forschungsgemeinschaft (Ma 1707/1-1 and Ma 1707/1-2 to U. M.) and by the Wellcome Trust (#060549 to U. M.).

REFERENCES

Bader, B. L., Rayburn, H., Crowley, D. and Hynes, R. O. (1998). Extensive vasculogenesis, angiogenesis, and organogenesis precede lethality in mice lacking all αv integrins. *Cell* **95**, 507-519.

Baumgartner, R., Czisch, M., Mayer, U., Pöschl, E., Huber, R., Timpl, R. and Holak, T. A. (1996). Structure of the nidogen binding LE module of the laminin γ1 chain in solution. *J. Mol. Biol.* **257**, 658-668.

Costell, M., Gustafsson, E., Aszodi, A., Mörgelin, M., Bloch, W., Hunziker, E., Addicks, K., Timpl, R. and Fässler, R. (1999). Perlecan maintains the integrity of cartilage and some basement membranes. *J. Cell Biol.* **147**, 1109-1122.

DiPersio, C. M., Hodivala-Dilke, K. M., Jaenisch, R., Kreidberg, J. A. and Hynes, R. O. (1997). α3β1 integrin is required for normal development of the epidermal basement membrane. *J. Cell Biol.* **137**, 729-742.

Dziadek, M. and Timpl, R. (1985). Expression of nidogen and laminin in basement membranes during mouse embryogenesis and in teratocarcinoma cells. *Dev. Biol.* **111**, 372-382.

Ekblom, P., Ekblom, M., Fecker, L., Klein, G., Zhang, H. Y., Kadoya, Y., Chu, M. L., Mayer, U. and Timpl, R. (1994). Role of mesenchymal nidogen for epithelial morphogenesis in vitro. *Development* **120**, 2003-2014.

Fox, J. W., Mayer, U., Nischt, R., Aumailley, M., Reinhardt, D., Wiedemann, H., Mann, K., Timpl, R., Krieg, T., Engel, J. and Timpl, R. (1991). Recombinant nidogen consists of three globular domains and mediates binding of laminin to collagen type IV. *EMBO J.* **10**, 3137-3146.

Halfter, W., Dong, S., Yip, L., Willem, M. and Mayer, U. (2002). A critical function of the pial basement membrane in cortical histogenesis. *J. Neurosci*. (in press).

Helbling-Leclerc, A., Zhang, X., Topaloglu, H., Cruaud, C., Tesson, F., Weissenbach, J., Tome, F. M., Schwartz, K., Fardeau, M., Tryggvason, K. and Guicheney, P. (1995). Mutations in the laminin α2-chain gene (LAMA2) cause merosin-deficient congenital muscular dystrophy. *Nat. Genet.* **11**, 216-218.

Henry, M. D. and Campbell, K. P. (1998). A role for dystroglycan in basement membrane assembly. *Cell* **95**, 859-870.

Hopf, M., Göhring, W., Kohfeldt, E., Yamada, Y. and Timpl, R. (1999). Recombinant domain IV of perlecan binds to nidogens, laminin-nidogen complex, fibronectin, fibulin-2 and heparin. *Eur. J. Biochem.* **259**, 917-925.

Jacob, M., Konrad, K. and Jacob, H. J. (1999). Early development of the müllerian duct in avian embryos with reference to the human. An ultrastructural and immunohistochemical study. *Cells Tiss. Organs* **164**, 63-81.

Kaartinen, V., Voncken, J. W., Shuler, C., Warburton, D., Bu, D., Heisterkamp, N. and Groffen, J. (1995). Abnormal lung development and cleft palate in mice lacking TGF-β3 indicates defects of epithelial-mesenchymal interaction. *Nat. Genet.* **11**, 415-421.

Kadoya, Y., Salmivirta, K., Talts, J. F., Kadoya, K., Mayer, U., Timpl, R. and Ekblom, P. (1997). Importance of nidogen binding to laminin γ1 for branching epithelial morphogenesis of the submandibular gland. *Development* **124**, 683-691.

Kallunki, T., Ikonen, J., Chow, L. T., Kallunki, P. and Tryggvason, K. (1991). Structure of the human laminin B2 chain gene reveals extensive divergence from the laminin B1 chain gene. *J. Biol. Chem.* **266**, 221-228.

Kang, S. H. and Kramer, J. M. (2000). Nidogen is nonessential and not required for normal type IV collagen localization in Caenorhabditis elegans. *Mol. Biol. Cell* **11**, 3911-3923.

Koch, M., Olson, P. F., Albus, A., Jin, W., Hunter, D. D., Brunken, W. J., Burgeson, R. E. and Champliaud, M. F. (1999). Characterization and expression of the laminin γ3 chain: a novel, non-basement membrane-associated, laminin chain. *J. Cell Biol.* **145**, 605-618.

Kohfeldt, E., Sasaki, T., Göhring, W. and Timpl, R. (1998). Nidogen-2: a new basement membrane protein with diverse binding properties. *J. Mol. Biol.* **282**, 99-109.

Kreidberg, J. A., Donovan, M. J., Goldstein, S. L., Rennke, H., Shepherd, K., Jones, R. C. and Jaenisch, R. (1996). α3β1 integrin has a crucial role in kidney and lung organogenesis. **122**, 3537-3547.

Lechner, M. S. and Dressler, G. R. (1997). The molecular basis of embryonic kidney development. *Mech. Dev.* **62**, 105-120.

Leveen, P., Pekny, M., Gebre-Medhin, S., Swolin, B., Larsson, E. and Betsholtz, C. (1994). Mice deficient for PDGF B show renal, cardiovascular, and hematological abnormalities. *Genes Dev.* **8**, 1875-1887.

Libby, R. T., Champliaud, M. F., Claudepierre, T., Xu, Y., Gibbons, E. P., Koch, M., Burgeson, R. E., Hunter, D. D. and Brunken, W. J. (2000). Laminin expression in adult and developing retinae: evidence of two novel CNS laminins. *J. Neurosci.* **20**, 6517-6528.

Mayer, U. and Timpl, R. (1994). Structure and function of basement membrane protein nidogen. In *Extracellular Matrix Assembly and Structure* (ed. P. D. Yurchenco, D. E. Birk and R. E. Mecham), pp. 383-416. San Diego, CA: Academic Press.

Mayer, U., Mann, K., Timpl, R. and Murphy, G. (1993a). Sites of nidogen cleavage by proteases involved in tissue homeostasis and remodelling. *Eur. J. Biochem.* **217**, 877-884.

Mayer, U., Nischt, R., Pöschl, E., Mann, K., Fukuda, K., Gerl, M., Yamada, Y. and Timpl, R. (1993b). A single EGF-like motif of laminin is responsible for high affinity nidogen binding. *EMBO J.* **12**, 1879-1885.

Mayer, U., Pöschl, E., Gerecke, D. R., Wagman, D. W., Burgeson, R. E. and Timpl, R. (1995). Low nidogen affinity of laminin-5 can be attributed to two serine residues in EGF-like motif γ2III4. *FEBS Lett.* **365**, 129-132.

Mayer, U., Saher, G., Fässler, R., Bornemann, A., Echtermeyer, F., von der Mark, H., Miosge, N., Pöschl, E. and von der Mark, K. (1997). Absence of integrin α7 causes a novel form of muscular dystrophy. *Nat. Genet.* **17**, 318-323.

Mayer, U., Kohfeldt, E. and Timpl, R. (1998). Structural and genetic analysis of laminin-nidogen interaction. *Ann. New York Acad. Sci.* **857**, 130-142.

Miner, J. H., Cunningham, J. and Sanes, J. R. (1998). Roles for laminin in embryogenesis: exencephaly, syndactyly, and placentopathy in mice lacking the laminin α5 chain. *J. Cell Biol.* **143**, 1713-1723.

Miner, J. H. and Patton, B. L. (1999). Laminin-11. *Int. J. Biochem. Cell Biol.* **31**, 811-816.

Mitchell, K. J., Pinson, K. I., Kelly, O. G., Brennan, J., Zupicich, J., Scherz, P., Leighton, P. A., Goodrich, L. V., Lu, X., Avery, B. J. et al. (2001). Functional analysis of secreted and transmembrane proteins critical to mouse development. *Nat. Genet.* **28**, 241-249.

Miyazaki, Y., Oshima, K., Fogo, A., Hogan, B. L. and Ichikawa, I. (2000). Bone morphogenetic protein 4 regulates the budding site and elongation of the mouse ureter. *J. Clin. Invest.* **105**, 863-873.

Moore, M. W., Klein, R. D., Farinas, I., Sauer, H., Armanini, M., Phillips, H., Reichardt, L. F., Ryan, A. M., Carver-Moore, K. and Rosenthal, A. (1996). Renal and neuronal abnormalities in mice lacking GDNF. *Nature* **382**, 76-79.

Müller, U. and Brändli, A. W. (1999). Cell adhesion molecules and extracellular-matrix constituents in kidney development and disease. *J. Cell Sci.* **112**, 3855-3867.

Müller, U., Wang, D., Denda, S., Meneses, J. J., Pedersen, R. A. and Reichardt, L. F. (1997). Integrin α8β1 is critically important for epithelial-mesenchymal interactions during kidney morphogenesis. *Cell* **88**, 603-613.

Murray, P. and Edgar, D. (2000). Regulation of programmed cell death by basement membranes in embryonic development. *J. Cell Biol.* **150**, 1215-1221.

Murshed, M., Smyth, N., Miosge, N., Karolat, J., Krieg, T., Paulsson, M. and Nischt, R. (2000). The absence of nidogen 1 does not affect murine basement membrane formation. *Mol. Cell. Biol.* **20**, 7007-7012.

Overton, J. (1959). Studies on the mode of outgrowth of the amphibian pronephric duct. *J. Embryol. Exp. Morphol.* **7**, 86-93.

Paulsson, M., Aumailley, M., Deutzmann, R., Timpl, R., Beck, K. and Engel, J. (1987). Laminin-nidogen complex. Extraction with chelating agents and structural characterization. *Eur. J. Biochem.* **166**, 11-19.

Pope, J. C., Brock, J. W., III, Adams, M. C., Stephens, F. D. and Ichikawa, I. (1999). How they begin and how they end: classic and new theories for the development and deterioration of congenital anomalies of the kidney and urinary tract, CAKUT. *J. Am. Soc. Nephrol.* **10**, 2018-2028.

Pöschl, E., Fox, J. W., Block, D., Mayer, U. and Timpl, R. (1994). Two non-contiguous regions contribute to nidogen binding to a single EGF-like motif of the laminin γ1 chain. *EMBO J.* **13**, 3741-3747.

Pöschl, E., Mayer, U., Stetefeld, J., Baumgartner, R., Holak, T. A., Huber, R. and Timpl, R. (1996). Site-directed mutagenesis and structural interpretation of the nidogen binding site of the laminin γ1 chain. *EMBO J.* **15**, 5154-5159.

Pulkkinen, L. and Uitto, J. (1999). Mutation analysis and molecular genetics of epidermolysis bullosa. *Matrix Biol.* **18**, 29-42.

Ries, A., Göhring, W., Fox, J. W., Timpl, R. and Sasaki, T. (2001). Recombinant domains of mouse nidogen-1 and their binding to basement membrane proteins and monoclonal antibodies. *Eur. J. Biochem.* **268**, 5119-5128.

Rodriguez-Boulan, E. and Nelson, W. J. (1989). Morphogenesis of the polarized epithelial cell phenotype. *Science* **245**, 718-725.

Sasaki, T., Wiedemann, H., Matzner, M., Chu, M. L. and Timpl, R. (1996).

Expression of fibulin-2 by fibroblasts and deposition with fibronectin into a fibrillar matrix. *J. Cell Sci.* **109**, 2895-2904.

Sasaki, T., Forsberg, E., Bloch, W., Addicks, K., Fässler, R. and Timpl, R. (1998). Deficiency of β1 integrins in teratoma interferes with basement membrane assembly and laminin-1 expression. *Exp. Cell Res.* **238**, 70-81.

Saxen, L. (1987). *Organogenesis of the Kidney.* Cambridge, UK: Cambridge University Press.

Shi, W., Heisterkamp, N., Groffen, J., Zhao, J., Warburton, D. and Kaartinen, V. (1999). TGF-β3-null mutation does not abrogate fetal lung maturation in vivo by glucocorticoids. *Am. J. Physiol.* **277**, L1205-L1213.

Schuchardt, A., D'Agati, V., Pachnis, V. and Costantini, F. (1996). Renal agenesis and hypodysplasia in ret-k- mutant mice result from defects in ureteric bud development. *Development* **122**, 1919-1929.

Smyth, N., Vatansever, H. S., Murray, P., Meyer, M., Frie, C., Paulsson, M. and Edgar, D. (1999). Absence of basement membranes after targeting the LAMC1 gene results in embryonic lethality due to failure of endoderm differentiation. *J. Cell Biol.* **144**, 151-160.

Stetefeld, J., Mayer, U., Timpl, R. and Huber, R. (1996). Crystal structure of three consecutive laminin-type epidermal growth factor-like (LE) modules of laminin γ1 chain harboring the nidogen binding site. *J. Mol. Biol.* **257**, 644-657.

Thomas, T. and Dziadek, M. (1993). Genes coding for basement membrane glycoproteins laminin, nidogen, and collagen IV are differentially expressed in the nervous system and by epithelial, endothelial, and mesenchymal cells of the mouse embryo. *Exp. Cell Res.* **208**, 54-67.

Timpl, R. and Brown, J. C. (1996). Supramolecular assembly of basement membranes. *BioEssays* **18**, 123-132.

Torres, M., Gomez-Pardo, E., Dressler, G. R. and Gruss, P. (1995). Pax-2 controls multiple steps of urogenital development. *Development* **121**, 4057-4065.

Vorbroker, D. K., Profitt, S. A., Nogee, L. M. and Whitsett, J. A. (1995). Aberrant processing of surfactant protein C in hereditary SP-B deficiency. *Am. J. Physiol* **268**, L647-L656.

Williamson, R. A., Henry, M. D., Daniels, K. J., Hrstka, R. F., Lee, J. C., Sunada, Y., Ibraghimov-Beskrovnaya, O. and Campbell, K. P. (1997). Dystroglycan is essential for early embryonic development: disruption of Reichert's membrane in Dag1-null mice. *Hum. Mol. Genet.* **6**, 831-841.

Wobus, A. M., Wallukat, G. and Hescheler, J. (1991). Pluripotent mouse embryonic stem cells are able to differentiate into cardiomyocytes expressing chronotropic responses to adrenergic and cholinergic agents and Ca^{2+} channel blockers. *Differentiation* **48**, 173-182.

Yang, J. T., Rayburn, H. and Hynes, R. O. (1995). Cell adhesion events mediated by alpha 4 integrins are essential in placental and cardiac development. *Development* **121**, 549-560.